Journal of Physics: Conference Series

PAPER • OPEN ACCESS

Assessing aerodynamic influences on offshore foundation design for large wind farms

To cite this article: K Z Wen *et al* 2024 *J. Phys.: Conf. Ser.* **2745** 012023

Assessing aerodynamic influences on offshore foundation design for large wind farms

K Z Wen[1], D Dehtyriov[1], B W Byrne[1]

[1] Department of Engineering Science, University of Oxford, Parks Road, Oxford OX1 3PJ, UK.

E-mail: kathy.wen@spc.ox.ac.uk

Abstract. An evaluation of the impact of aerodynamic interactions on offshore wind turbine (OWT) monopile design in large wind farms is presented. The interactions between turbines within a wind farm, and between the atmosphere and the entire wind-farm, act to reduce the mean effective loads across the farm. This reduction impacts the operational performance of OWT foundations in two notable ways: a decrease in turbine structural loads which affects design to serviceability limit state and a shift in excitation frequencies of the passing blades which impacts fatigue performance. To assess the implications on monopile design, we conduct static and dynamic analyses using a 1-D finite element model (FEM). We show that the farm-atmosphere interaction effect leads to marked reduction in monopile lengths between $\sim 5-25\%$ across an entire wind farm. The dynamic analysis reveals a competing balance between shifting frequency bands and reduced wind loads on the fatigue response. The monopile design is found to be strongly dependent on wind farm size and ratio of wind to wave loading, with wave loading coupled to the farm-atmosphere interaction effect. Exploiting these interactions plays a pivotal role in reducing the levelised cost of wind energy and ensuring robust design of OWTs.

1. Introduction

Global wind turbine development is rapidly growing to meet renewable energy demands. As the wind energy industry has expanded, wind farm clusters have moved from onshore to offshore, and the size, number of turbines and mean water depth of these farms is expected to continue increasing over the coming decades. A driving factor contributing to this expansion is the falling cost of wind energy through increases in energy production efficiency and decreases in capital and operational expenditure. Optimisation of the design methods and technology for offshore wind farms is therefore a key ingredient in meeting both low carbon and energy security objectives.

Each turbine in a wind farm comprises a rotor and nacelle to extract power and a tower and foundation to transfer loads to founding soil. Modelling and optimising wind farms requires a detailed understanding of each sub-system and the ways in which they interact. We focus on the influence of aerodynamic interaction on the design of foundations for large offshore wind farms.

The majority of current offshore developments make use of a monopile foundation, which makes up one of the largest portions of capital expenditure. These foundations are individually designed for each turbine in the farm, with upwards of 40% variation in foundation mass across a single farm [1]. There are three variables which require optimisation for each turbine; length, L_p, wall-thickness, t_p and diameter, D_p. These variables depend on location specific meteorological conditions, turbine loads, sea-depth and soil properties. The limit states which decide these

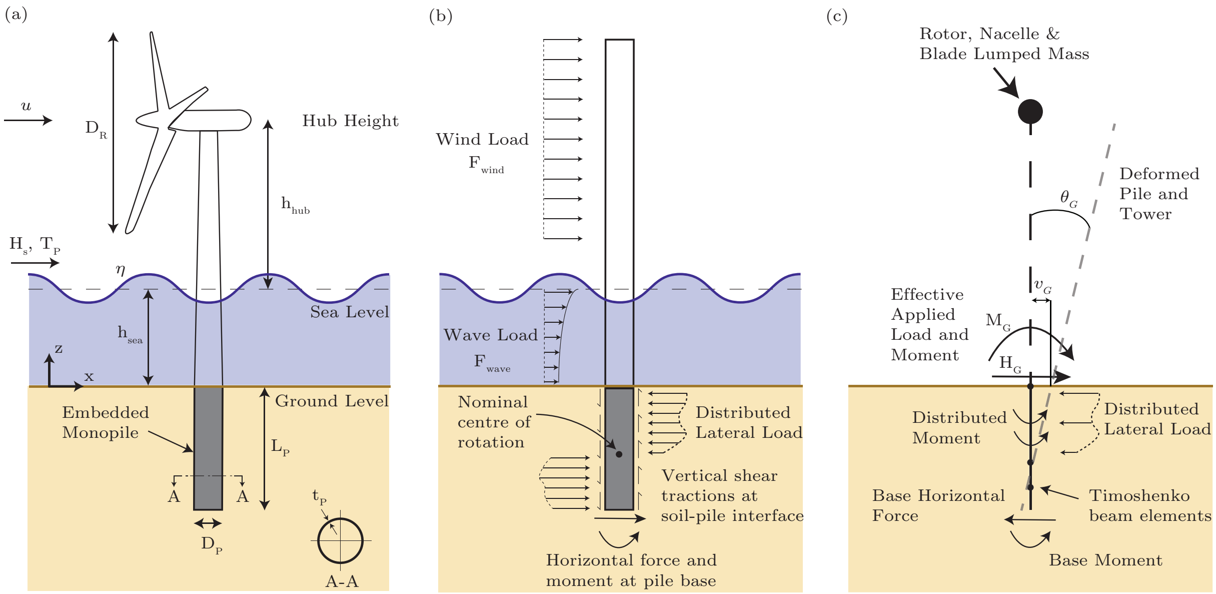

Figure 1: Schematic of the coupled load-monopile design problem. (a) Geometry of an OWT with monopile.(b) Simplified free-body diagram showing the distributed loads, and the balancing distributed soil-structure loads. (c) 1-D modelling of the system based on the PISA method.

designs are governed by installation, extreme weather events and loads under 'operational' conditions [2]. These loads include environmental loads i.e. wind and wave loading and cyclic operational loads caused by the rotation of the blades passing [3].

The characterisation of environmental and operational loads is incomplete due to aerodynamic interaction between individual wind turbines and between the wind farm and the atmospheric boundary layer. Each operating turbine locally reduces the wind speed and increases the turbulence in its wake. These wakes interact with other turbines, leading to power losses, upwards of 40% across a farm [4]. This effect, known as the wake effect, has been extensively explored, with models developed to quantify its impact. A recent observation has additionally identified a 'farm-atmosphere interaction' effect, where flow resistance caused by large wind farms reduces the wind speed upstream and within the farm [5]. Neglecting the farm-atmosphere interaction effect has historically led to a non-negligible bias in the wind resource assessment and has further implications for foundation design which forms the focus of this paper.

Engineering wake models approximating the relevant aerodynamics are extensively applied to estimate the net power production of a wind farm, determine wind farm control strategies [6], solve the wind farm layout optimisation problem [7], and estimate project costs and profit. Recently, the effects of turbine-wake interactions on foundation loads has additionally been identified [8]. However, an evaluation of the effects of farm-atmosphere interaction on foundation design is not presented in the literature thus far. In this paper, we investigate the implications of turbine-wake and farm-atmosphere interaction effect on monopile design by considering a simple wind turbine optimisation problem illustrated in figure 1. Both turbine-wake and farm-atmosphere interaction effects act to reduce the mean loads seen by turbines which subsequently influences their optimal design. We demonstrate that considering farm-atmosphere interaction effects significantly influences monopile design under both serviceabilty limit state (SLS) and fatigue limit state (FLS) design, especially as wind farms grow in size.

Table 1: IEA 15MW turbine parameters [11], herein used as the benchmark case.

Rotor Diameter	D_R (m)	240
Hub Height	h_{hub} (m)	150
Mean Sea Level	h_{sea} (m)	30
Rated Wind Speed	u_0 (m/s)	10.59
Design Thrust Coefficient	C_T	0.804
Design Power Coefficient	C_P	0.489
Design Tip Speed Ratio	TSR	9
Monopile diameter	D_P (m)	10
Monopile wall thickness	t_P (mm)	55

Table 2: IEA 15MW lumped mass structural properties [11]

.

		Nacelle	**Hub**
Lumped mass	m (t)	821	196
Offset from lumped mass about x-axis	x_{off}(m)	5.486	10.6
Offset from lumped mass about z-axis	z_{off}(m)	3.978	5.462
Moment of inertia x-axis	I_{xx} (tm^2)	12607	303000
Moment of inertia y-axis	I_{yy} (tm^2)	21434	152000
Moment of inertia z-axis	I_{zz}(tm^2)	18682	152000

2. Methodology

Consider the monopile design problem illustrated in figure 1a. The OWT rotor sees an incoming wind speed u across the rotor diameter D_R at height h_{hub}. The significant wave height H_S and peak spectral period T_P govern wave dynamics, with local sea free surface elevation η and mean sea-level elevation h_{sea}. The rotor is supported by a tower and embedded in the soil is a monopile. A simplified load representation of this problem is presented in figure 1b. The wind load is assumed uniformly distributed across a region bounded by the rotor, centered about h_{hub}. The wave load is distributed over the tower base between the ground and sea level η, assumed to act in the same direction as the wind load. The monopile resists loads under soil-structure interaction. We further simplify the load state to the 1-D representation illustration in figure 1c. The nacelle, hub and blades are modelled by a lumped mass. The monopile is modelled as a 1-D discretised beam. At each node, the soil-structure interaction is modelled as an independent non-linear spring, calibrated against 3-D finite element simulations and validated through field tests, see [9, 10] for details. We evaluate aerodynamics influences on monopile design considering the IEA 15MW reference turbine detailed in [11], with relevant parameters in table 1. Although specific loading cases, atmospheric conditions, wind farm size, soil conditions, blade designs and layouts determine precise design, the broader conclusions are independent of the reference case.

2.1. Load determination

To estimate the static wind load, we assume that the OWTs are operating in region II (above cut-in and below rated u) of the wind speed curve, representative of operating conditions, where the wind load varies quadratically with u

$$F_{\text{wind}} = \frac{1}{2}\rho u^2 A_T C_T. \tag{1}$$

where ρ is the air density, A_T is the rotor swept area and C_T the design rotor thrust coefficient. Dynamic analysis requires the calculation of turbulent wind kinematics which are added to the mean u, based on a Kaimal spectrum following the methodology presented in[12].

To estimate the static wave load, we approximate H_S and T_S by linearly interpolating wave conditions in [11] to the relevant u. The wave load estimation is based on Morrison's equation [13], where linear wave (Airy) theory is used to approximate the wave geometry. The mean horizontal velocity component of a wave propagating is

$$v_x = \frac{H_S g k}{2\omega}\frac{\cosh\left(k(z+h_{\text{sea}})\right)}{\cosh\left(kh_{\text{sea}}\right)}\cos\left(kx-\omega t\right), \tag{2}$$

where k is the wavenumber, determined from $\omega^2 = gk\tanh kh_{\text{sea}}$, $\omega = 2\pi/T_P$ is the wave frequency. The wave force on each element of the tower is determined by Morrison's equation

$$dF = dF_D + dF_I = \frac{1}{2}C_D\rho D v|v|dz + C_M\rho\frac{\pi D^2}{4}\dot{v}dz, \tag{3}$$

where the drag and inertial coefficients are assumed $C_D = 1$ and $C_M = 2$ respectively. The maxima of drag and inertial force terms are out of phase, we evaluate the two separately and sum them linearly. The forces are found by integrating equation 3

$$F_{\text{wave}} = \int_{-h_{\text{sea}}}^{\eta} dF_D + \int_{-h_{\text{sea}}}^{\eta} dF_I, \tag{4}$$

$$M_{\text{wave}} = \int_{-h_{\text{sea}}}^{\eta} dF_D(h_{\text{sea}}+z) + \int_{-h_{\text{sea}}}^{\eta} dF_I(h_{\text{sea}}+z), \tag{5}$$

where the local maxima of inertial load occurs for $t = 0$, $\eta = 0$, and for drag load for $t = T_P/4$, $\eta = H_S/2$. Aerodynamic interaction affects wind and wave loads differently, see sections 3-4. As such, We additionally consider the limiting case where $F_{\text{wave}} = M_{\text{wave}} = 0$ such that $F_{\text{wind}}/F_{\text{wave}} \to \infty$ to quantify the impact of variations in this ratio.

For the dynamic analysis, wave kinematics calculation based on [14] are undertaken. The Jonswap spectrum is used to estimate H_S and T_P based on u and estimated fetch [15].

Operational loads, 1P and 3P are caused by mass and aerodynamic imbalance of the rotor and by wind shear and tower shadow effects as blades pass the tower respectively. The 1P frequency ranges (f_{1P}) of the IEA 15MW turbine are determined from the tip speed ratio (TSR)

$$f_{1P} = \frac{\lambda u}{\pi D_R}, \tag{6}$$

where λ is the TSR. The 3P freqeuncy ranges is $f_{3P} = 3f_{1P}$. The magnitude of the tangential forces associated 1P and 3P $m_b u\lambda \approx 6$MN in region II, where the blade mass $m_b = 65$t.

2.2. Soil profile

The primary soil profile considered herein is Dunkirk sand, a dense marine sand profile heavily characterised for several field testing campaigns [16]. The sand stiffness profile is modelled by the relationship proposed by [17]

$$G_0 = \frac{Bp'_{\text{ref}}}{0.3+0.7e_0^2}\sqrt{\frac{p'}{p'_{\text{ref}}}} = m\sqrt{z}, \tag{7}$$

where the p' is mean effective stress variation with soil depth, $e_0 = 0.629$ (for a relative density of $D_{\text{Rel}} = 75\%$), $\gamma' = 10.09\text{kN/m}^3$, $B = 875$ and $p'_{\text{ref}} = 101.3$kPa. As a soil sensitivity study, we consider variations in m (equivalent to variations in B), and comparisons to an overconsolidated glacial clay till profile, with properties described in [18, 19].

2.3. Design methodology
We are concerned with design of OWT monopiles under SLS and FLS. Typically, SLS limits $D_P/10$ to the ground displacement v_G, and $0.5°$ to ground rotation θ_G, which are applied herein. FLS requires the natural frequency f_0 of the OWT to be desined designed to sit between rotor vibration (f_{1P}) and blade passing (f_{3P}) excitation frequency ranges, known as the "soft-stiff" region to avoid resonance and structural degradation [20].

The loads and soil profile are inputs to an in-house 1-D finite element model (FEM), referred to as OxDyn, described in[21]. The nacelle, hub and blades are modelled by a lumped mass with properties in table 2. The monopile is represented as a series of interconnected 1-D Timoshenko beam elements, (see figure 1c). The resultant finite-element equations are solved for v_G and θ_G of each beam element. This approach is described in [9, 10]. The dynamic fatigue assessment further requires the time integration calculation of the OWT response to a time varying load excitation (from wind, waves and 1P/3P loads). The dynamic response is solved by forward integration using the non-linear Newmark-beta method, obtaining the time-series load and displacement distribution at each beam element.

Turbine-wake and farm-atmosphere interaction effects decrease mean u and loads seen by OWTs. The aerodynamic load scales quadratically with reduction in u through equation 1, where $u = \beta u_0$, β is the wind speed reduction factor. For turbine-wake interaction, the wave load is assumed unaffected, for farm-atmosphere interaction effects, updated wave loads are computed for new u through equations 4-5.We assume a fixed D_p and vary L_p in response to changes in load. The 1-D FEM is solved iteratively for minimum L_p to satisfy SLS conditions.

FLS is constrained by f_0, determined by eigenvalues analysis, solving the following simplified characteristic equation for values of undamped natural frequencies, f_n

$$(\mathbf{K} - (2\pi f_n)^2\mathbf{M})x \sin(2\pi f_n t) = 0, \tag{8}$$

where $\mathbf{K}$ and $\mathbf{M}$ are the stiffness and mass matricies respectively, x is the displacement vector, f_0 is the first dominant modal frequency. The proximity of f_0 to f_{1P} and f_{3P} dictates the amount of fatigue damage. Based on the assumption of linear cumulative damage, the fatigue life of structures may be calculated based on the S-N fatigue approach (Palmgren-Miner rule) [22]. The accumulated damage D, represents the ratio of number of cycles accumulated for a given stress range to the total number of cycles to failure for the same stress range and is determined by equation 9 described in[23]

$$D = \sum_{i=1}^{k} \frac{n_i}{N_i} = \frac{1}{\bar{a}} \sum_{i=1}^{k} n_i \dot{(}\Delta\sigma_i)^m, \tag{9}$$

where $\bar{a}$ is the intercept of the S-N curve with the $\log N$ axis, m is the negative inverse slope of the S-N curve, k is the number of stress blocks, n_i is the number of stress cycles in each block i, computed from the time-series input from dynamic analysis and N_i is the number of cycles to failure at constant stress range $\Delta\sigma_i$. Failure is assumed to occur in the butt welds at ground level where bending moment is the highest, with the S-N curves provided in DNV-RP-C203 [23].

3. Turbine wake interaction effect
Across a wind farm, the first column of turbines see the upstream meteorological u, however, turbines deeper in the farm experience a significant reduction in u and load due to turbine-wake interactions. For large farms, the majority of turbines will experience similar levels of reduced load, except the first few columns.

We focus on expected normalised wake losses at the Horns Rev wind farm based on experimentally measured results presented in [4], although engineering wake models such as

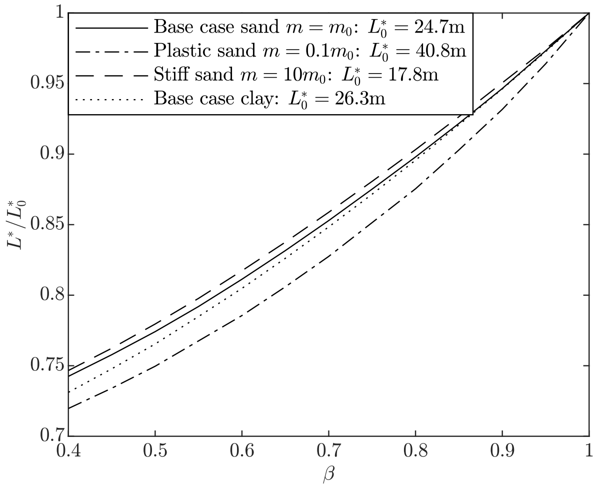

Figure 2: Soil sensitivity study relating the aerodynamic impact, characterised by β on L_p variation L^*/L_0^* for various soil profiles. The base case sand is compared to a clay profile [19], and the proportionality constant m for the base case sand (see equation 7) is varied in both directions and compared. Over a large range of β and soil strengths, the mean L_p reductions are relatively insensitive to the soil profiles.

the Jensen model can be used as a first-order prediction instead. In particular, we focus on the mean power reduction across the range of wind directions considered in [4], and changes in mean u seen by turbines as a function of their depth within the farm.

Since far-wake velocity deficits are unaffected by specifics of OWT blade design [24], and primarily depend on C_T, we assume normalised power losses in [4] are reasonable approximations of expected turbine-wake losses and apply the same β for the IEA 15MW turbine presented herein, assuming turbine-wake interactions have no impact on the wave load.

Figure 2 presents the results for the IEA 15MW. The difference in soil profiles impact nominal L_p, however changes to L_p is insensitive to soil type. For a two order magnitude change in soil stiffness, and $\beta = 0.4$, the difference in relative L_0^* remains below 3%. The influence of turbine-wake effects on monopile design is considered insensitive to realistic variations in soil conditions.

Across wind directions (figure 3a), mean reduction to $L_p \approx 5\%$. Reductions are not uniformly distributed, and depend on the 'depth' of each turbine in the farm and wind direction. For wind direction corresponding to the least wake interaction (figure 3b), L_p decreases near linearly with distance into the farm. For the worst-case scenario (figure 3c) where the turbine array is aligned with wind direction, turbines in the first wind-facing column require an increased L_p, and mean L_p reduction for other turbines is $\approx 7\%$. As wind farms grow, plateaus in L_p are expected for all wind directions; for medium sized farms, considering wake interaction in monopile design requires additional coupling to u and direction joint probability distributions [25].

The ratio of wind to wave loads emerges as a critical parameter that controls the relative impact of turbine-wake interactions on monopile design. It is anticipated that the significance of these impacts will increase as OWTs grow. Likewise, if operating in a sea-state with low wave loading, aerodynamic interaction effects increase in significance. As demonstrated in figure 3, in the limiting case where the wave loads are negligible compared to the wind load, the mean L_p reduction across the farm falls from 5% to 8% (figure 3a), with larger variation across changing wind directions. Turbines 'deeper' in the farm see a significant reduction in L_p (figures 3b-c), with reduction approaching 15% for both best and worst case wind alignment scenarios.

4. Farm-atmosphere interaction effect

As the size of wind farms increase, changes to mean u and thus monopile design become governed by farm-atmosphere interaction effects. A numerical weather prediction model simulation used to compare atmospheric flow with and without a wind farm present is presented in [26], and illustrates velocity slow down across an entire wind farm as response to the presence of a wind farm. The β is independent of turbine layout and instead depends on interaction between

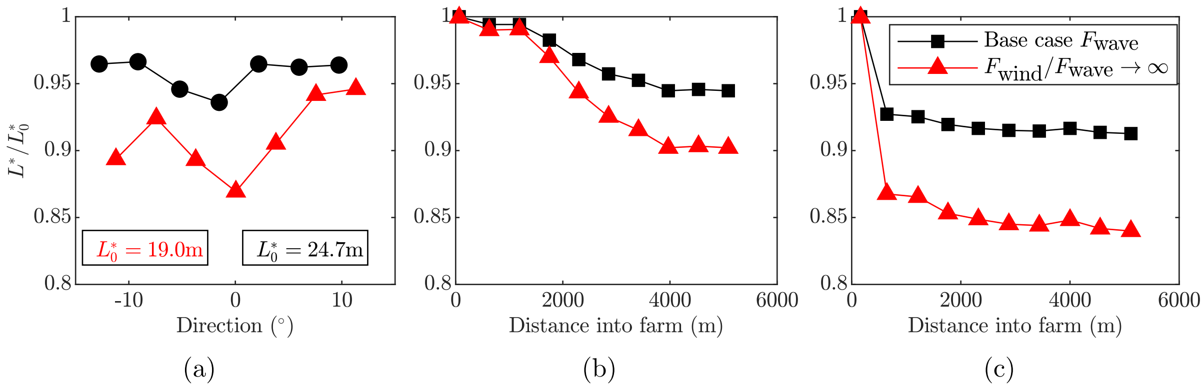

Figure 3: Reduction in optimal L_p for two wind to wave loading ratio cases, due to turbine-wake interaction effects measured at the Nysted wind farm, with larger reductions for a given loading corresponding to increased wake-turbine interactions. (a) The mean farm-wide reduction variation with wind direction. (b), (c) L_p variation with distance into the farm for the wind directions with minimum wake interaction and maximum wake interaction respectively.

the wind farm and atmospheric boundary layer. A two-scale theoretical model predicting the velocity slowdown for fully developed wind farms was presented by [27], after it was observed to impact power predictions for current wind farms [5]:

$$4\alpha(1-\alpha)\frac{\lambda}{C_{f0}}\beta_f^2 + \beta_f^\gamma = M, \tag{10}$$

where we assume $\gamma = 2$ based on [27], with the results relatively insensitive to this parameter, and the momentum availability factor M is modelled as a linear approximation which has been shown to work well over a practical range of β_f [26]

$$M = 1 + \zeta(1-\beta_f). \tag{11}$$

Equation 10 relates the turbine-scale flow physics, 'internal' conditions (e.g, the turbine layout and operating conditions) on the left-hand side, to the interaction between the wind farm and atmospheric boundary layer, 'external' conditions, on the right-hand side. Equations 10-11 are solved for farm flow velocity slowdown due to farm-atmosphere interaction β_f assuming turbines operate at maximum efficiency ($C_P = 4\alpha^2(1-\alpha)\beta_f^3$). We note turbine operating points can be adjusted to mitigate some of the farm-atmosphere interaction effects [28] which could be considered in a detailed design.

The theoretical model predicts the global velocity deficit based on; the momentum response parameter ζ, an empirically determined parameter which relates the extracted momentum from the atmosphere due to the presence of the farm with the mean velocity reduction, and the effective array density λ/C_{f0}, where $\lambda = nA_R/S_F$ (n is the number of turbines, A_R the swept area of the turbine and S_F the wind farm area) and C_{f0} is the sea-surface friction coefficient (typically $C_{f0} \approx 0.002$). For an infinitely large wind farm, $\zeta = 0$, ζ increases exponentially with decreasing wind farm size. Further details of the theoretical modelling are presented in [27].

For a specific wind farm site and layout, numerical weather simulations are required to determine precise extractability factor and turbine-wake interaction estimates; here, we seek a first order estimate to expected impacts, and to demonstrate their significance. To understand the joint effect of turbine-wake interaction and farm-atmosphere interaction effects, [29] simulated wind farms varying layouts over the ζ-λ/C_{f0} space. The relative impact of the

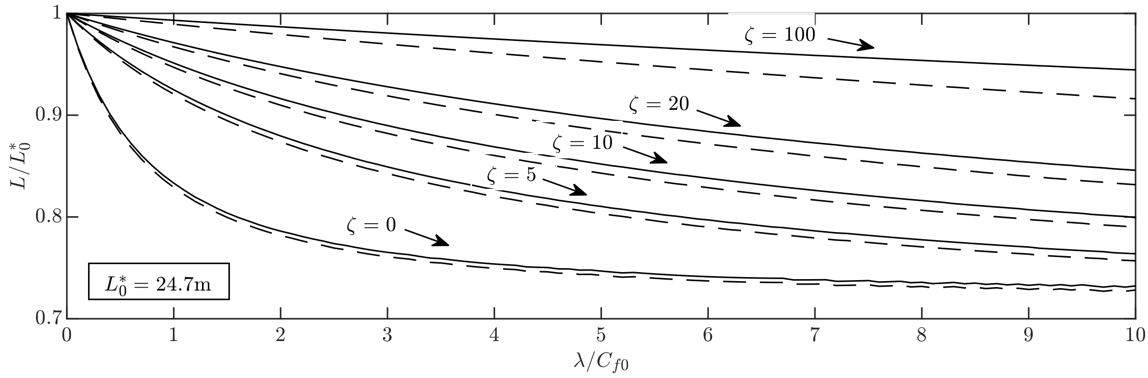

(a)

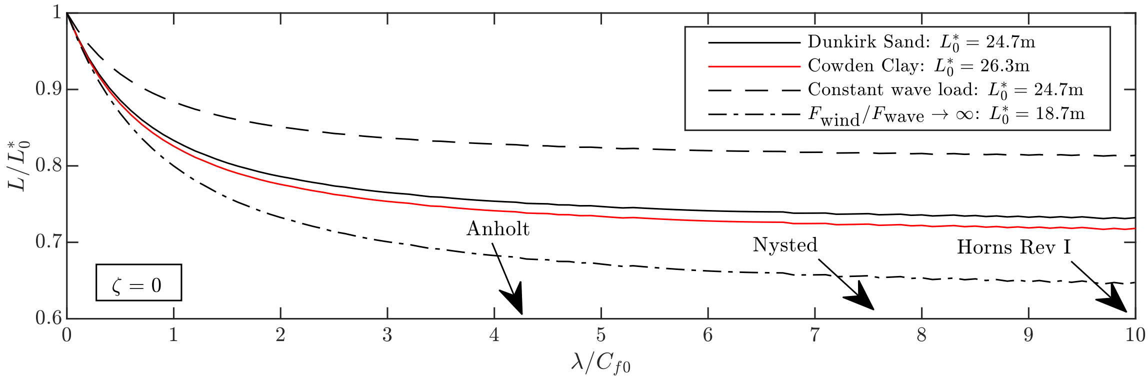

(b)

Figure 4: Reduction in optimal L_0^* under aerodynamic coupling, parametrised against the momentum extractability factor ζ, and effective array density λ/C_{f0} (approximate λ/C_{f0} for wind farms indicated). (a) The base case, assuming wave loads are altered by farm-atmosphere interaction, for a range of ζ. The solid lines show farm-atmosphere interaction effect only, the dashed lines show combined turbine-wake and farm-atmosphere effect impact. (b) Solutions for an infinitely large wind farm ($\zeta = 0$). The solid curves show the base reference case, assuming wave loads are affected by farm-atmosphere interaction, with black red lines indicating Dunkirk sand and Cowden clay respectively. The dashed curve shows the solution assuming farm-atmosphere interaction effect does not affect wave loading, and the dash-dotted line assumes the wave loading is negligible compared to the wind loading.

turbine-wake effect is estimated by averaging the results presented in [29] for $\lambda/C_{f0} \leq 10$ over the range of ζ presented, which exhibits a near linear relationship. This linear fit is used to estimate turbine-wake impact, the theoretical model in [27] is employed to estimate the farm-wide impact.

The farm-scale aerodynamic interaction decreases the mean u within and upstream of the entire wind farm to a larger scale compared to turbine-wake interactions. Wind-generated waves are assumed to adjust in H_S and T_S based on the new mean u, according to section 2. Consequently, the farm-atmosphere effect reduces both the wind and wave loads.

Figure 4a presents the results demonstrating significant farm-atmosphere interaction impact on monopile design. In the limiting case of a very large wind farm ($\zeta = 0$), and for realistic λ/C_{f0}, the mean L_p is reduced by upwards of 25%. Here, farm-atmosphere interaction dominates the turbine-wake effect, and monopile designs are insensitive to turbine layout and wind direction.

As ζ increases, and wind farms become smaller, the relative importance of turbine-wake

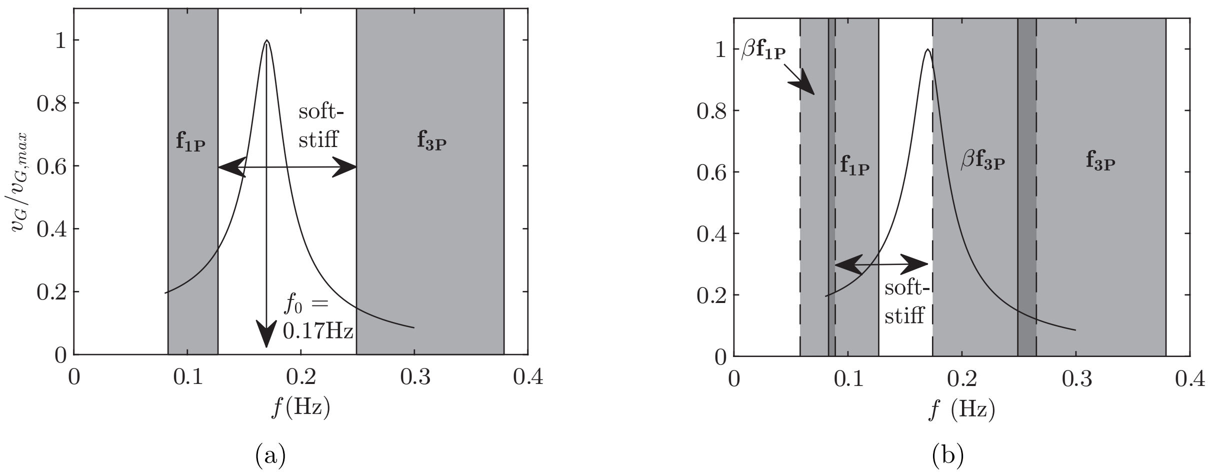

Figure 5: v_G response of the IEA 15MW turbine ($L_0^* = 24.7m$) with excitation frequency (a) The reference case $\beta = 1$ (b) $\beta = 0.7$. The shaded regions represent the f_{1P} and f_{3P} ranges.

aerodynamics grow, at $\zeta = 100$, the impact of farm-atmosphere and turbine-wake effects approximately balance. For small wind farms, load considerations are predominantly influenced by turbine-wake interaction, however, as wind farms expand, the governing factor shifts to farm-atmosphere interaction.

The results show that the convexity of the relationship between λ/C_{f0} and L_p reduction changes with farm size. For small farms, λ/C_{f0} has a near linear relationship with L_p reduction, therefore doubling the number of turbines approximately doubles the relative L_p reduction. For larger farms, increasing the number of turbines at low densities will have an appreciable impact on the permissible change in mean L_p. As more turbines are added to the farm, L_p decreases until the addition of further turbines no longer impacts monopile design.

Soil conditions do not significantly influence L_p reduction (figure 4b). Instead, the ratio of wind to wave loads is critical in evaluating the aerodynamic impact on monopile design. We explore two modifications to the base assumptions; the first where the u reduction under farm-atmosphere interaction has no impact on H_S and T_S (and therefore wave loads); and second where wave loads are negligible compared to wind loads. These scenarios highlight the importance of considering the combined effect of wind and wave loads on monopile design.

The ratio of wind to wave loading decreases with increasing λ/C_{f0} as only wind loads decrease. The plateau in L_p drops from 25% to near 15%. Contrariwise, for a negligible wave load, this plateau increases to 35%. A detailed understanding of the response of wave loads to the presence of a wind farm is thus critical to the optimisation of offshore monopile design.

As both wind farms and wind turbines continue to increase, the farm scale aerodynamic physics are expected to have a more pronounced impact on reduction on mean u and hence in the optimisation of monopile design. It has been shown that farm-atmosphere interaction effects have substantial implications regarding reduction in L_p for large wind farms.

5. Natural Frequency and Fatigue

The implication of turbine-wake interaction and farm-atmosphere interaction on the fatigue performance of OWTs are now discussed. The v_G response of the IEA 15MW turbine across a range of excitation frequencies is shown in figure 5a.

As anticipated, the excitation frequency at $f = f_0$ results in the largest v_G. The optimal TSR for power production depends on the turbine diameter and blade lift-to-drag ratios and is constant in region II, where the turbine operates the majority of the time. In the other

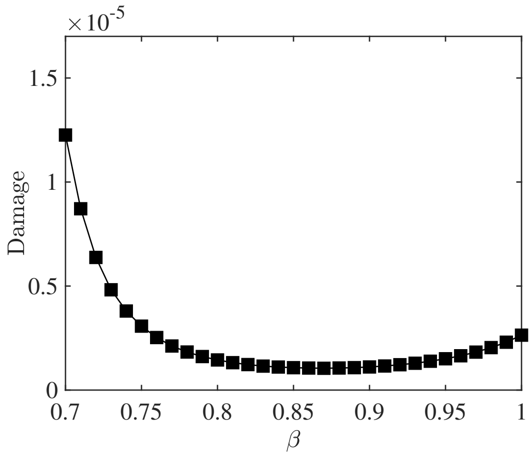

(a)

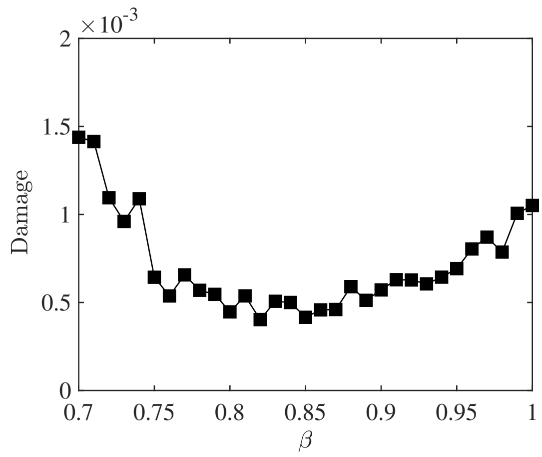

(b)

Figure 6: Damage response as a function of β calculated for a 10 minute time interval by (a) 1P and 3P loads and (b) combined environmental and operational loads.

operational regions, the TSR is varied to limit power production and rotation speed and avoid damage to the turbine [11]. For scope, we only consider changes in β on fatigue impact, however we note that the turbine-wake interaction additionally increases the mean turbulence levels across the farm. For a reduction in mean u across the farm and constant TSR, the f_{1P} and f_{3P} bands shift by a factor β (see equations 6) to maintain optimal aerodynamic efficiency. This shift is illustrated in figure 5b, where as β decreases, the "soft-stiff" region also decreases both in nominal value and in range. As the "soft-stiff" region shifts to lower frequencies, the amount of v_G (a proxy for damage) increases as represented by the area under the curve.

The influence of the reduced u on the damage response caused by isolated 1P/3P loads and combined environmental and operational loads are shown in figures 6(a, b) respectively.

Here it is demonstrated that reduction in u largely influences the damage response caused by 1P/3P loads, see Figure 6a. Damage by 1P/3P increases rapidly as β reduces due to the reduction of the 3P region interfering with f_0 as shown in figure 6b. However, the influence of β on the combined damage response from all loads produces a varied response. Under all loading, the damage to the OWT decreases for small for $\beta \leq 0.85$, this is attributed to the decrease in damage from the wind load from reduced u. Further reduction in β however shows that damage from the 1P/3P loads counteracts the beneficial effect of decreased wind load. As the 3P region shifts closer to f_0 greater damage to the OWT is observed. For u reductions associated with large wind farms (farm-atmosphere interaction considerations), a re-design of the monopfile may be necessary to maintain the fatigue performance of the OWT. Eigenvalue analysis indicates that changes to L_p do not greatly influence f_0 within typical L/D ratios of OWTs, corroborated by [30]. Variation in t_p is therefore necessary to counteract the aerodynamic effects ensuring f_0 remains within the "soft-stiff" region. The optimal value of t_p will depend on the site specific atmospheric characteristics, soil profile and turbine attributes. OWT foundation designers need to consider all these factors to ensure robust fatigue design for large wind farms.

6. Conclusion

The implications of aerodynamic interactions on monopile design for large wind farms has been explored in this study. Two aerodynamic phenomena are known to impact the mean loads and excitation frequencies seen by wind turbines across a farm; turbine-wake interaction physics where turbulent wakes behind turbines interact with other turbines in the farm, and farm-atmosphere interaction, where the whole wind farm resists the atmospheric flow. The changes to mean loading is coupled to a 1-D FEM where the static and dynamic response of an OWT is considered to investigate the magnitude of expected impact of aerodynamics on monopile design.

The turbine design and environmental data is taken from the IEA 15MW OWT [11]. Two soil profiles are considered; a cohesionless sand and a cohesive clay, representative of typical offshore soil profiles and characterised for the PISA project [16]. To understand the sensitivity of our results to soil stiffness, we varied soil stiffness by an order of magnitude in both directions. To quantify the impact of turbulent wake interaction, we used experimental data from the Horns Rev wind farm [4]. For the farm-atmosphere scale impact, we coupled our monopile design methodology with the two-scale flow theory presented in [27]. Finally, we considered the combined impact of both aerodynamic effects using simulation data presented in [29]. The first-order analysis assumes a fully developed wind farm with uniform unsheared flow.

For any given loading condition, L_p is minimised to satisfy SLS. Dynamic analyses are performed to evaluate the effect of turbine-wake and farm-atmosphere interaction on f_0 and subsequently the fatigue performance of OWTs. The results indicate that accounting for the turbine and farm-atmosphere aerodynamic effects significantly reduces the required mean L_p to satisfy SLS by $\sim$ 5% upwards 25%. These reductions become more pronounced for large wind farms where farm-scale aerodynamics dominate the turbine-wake interaction effects. Simultaneously fatigue analysis demonstrates that a re-design of t_p may be necessary to ensure the f_0 of the system remains between the f_{1P} and f_{3P} to maintain adequate fatigue performance. However this heavily depends on wind farm specific characteristics. For small changes to incoming mean wind speed such as those induced by turbine-wake interactions, the fatigue performance of the OWT increases directly as a results of wind load reduction. For large wind farms, where farm-atmosphere aerodynamics dominate, the fatigue performance decreases due to the f_{3P} region interfering with f_0, necessitating a re-design of t_p. The farm-atmosphere interaction effect is additionally expected to reduce H_S as the mean atmospheric u is reduced by the farm-atmosphere interaction. The ratio of wind to wave loading is a critical parameter in estimating the influence of the changes in environmental load on monopile design.

Neglecting these aerodynamic interactions not only results in overly conservative monopile design but also can lead to unaccounted structural fatigue damage. These effects are expected to become more pertinent as individual wind turbine sizes increase and wind farms grow in size. Establishing a framework which integrates the aerodynamic interactions with foundation design is crucial for robust performance of OWT and ongoing reductions in the levelised cost of energy. Turbine manufacturer's will need to further collaborate with wind farm developers to ensure that these components of wind farm design are appropriately modelled in future.

References

[1] Kallehave D, Byrne BW, LeBlanc TC, Mikkelsen KK. Optimization of monopiles for offshore wind turbines. Philosophical Transactions of the Royal Society A: Mathematical, Physical and Engineering Sciences. 2015;373(2035):20140100.

[2] Det Norske Veritas and Germanischer Lloyd. Support structures for wind turbines. DNV GL; 2016. 0126.

[3] Nikitas G, Vimalan N, Bhattacharya S. An innovative cyclic loading device to study long term performance of offshore wind turbines. Soil Dynamics and Earthquake Engineering. 2016 03;82:154-60.

[4] Barthelmie RJ, Pryor SC, Frandsen ST, Hansen KS, Schepers JG, Rados K, et al. Quantifying the impact of wind turbine wakes on power output at offshore wind farms. Journal of Atmospheric and Oceanic Technology. 2010;27(8):1302-17.

[5] Bleeg J, Purcell M, Ruisi R, Traiger E. Wind Farm Blockage and the Consequences of Neglecting Its Impact on Energy Production. Energies. 2018 Jun;11(6):1609.

[6] Shapiro CR, Starke GM, Meneveau C, Gayme DF. A Wake Modeling Paradigm for Wind Farm Design and Control. Energies. 2019;12(15).

[7] Park J, Law KH. Layout optimization for maximizing wind farm power production using sequential convex programming. Applied Energy. 2015;151:320-34.

[8] Larsen G, Larsen T, Pedersen M, Enevoldsen K, Aagaard Madsen H. Wake affected offshore tower and foundation loads. No. 131 in DTU Wind Energy E. Denmark: DTU Wind Energy; 2016.

[9] Byrne BW, Houlsby GT, Burd HJ, Gavin KG, Igoe DJP, Jardine RJ, et al. PISA design model for monopiles for offshore wind turbines: application to a stiff glacial clay till. Géotechnique. 2020;70(11):1030-47.

[10] Burd HJ, Taborda DMG, Zdravković L, Abadie CN, Byrne BW, Houlsby GT, et al. PISA design model for monopiles for offshore wind turbines: application to a marine sand. Géotechnique. 2020;70(11):1048-66.

[11] Evan G, Rinker J, Sethuraman L, Zahle F, Anderson B, Barter G, et al. Definition of the IEA 15-Megawatt Offshore Reference Wind. Golden, CO, USA: National Renewable Energy Laboratory; 2020. NREL/TP-5000-75698.

[12] International Electrotechnical Commission. Wind energy generation systems - Part 1: Design requirements. IEC; 2019. IEC 61400-1.

[13] Morison J, Johnson JW, Schaaf SA. The force exerted by surface waves on piles. Journal of Petroleum Technology. 1950;2(05):149-54.

[14] International Electrotechnical Commission. Wind energy generation systems - Part 3-1: Design requirements for fixed offshore wind turbines. IEC; 2019. IEC 61400-3.

[15] Hasselmann K, Barnett TP, Bouws E, Carlson H, Cartwright DE, Enke K, et al. Measurements of wind-wave growth and swell decay during the Joint North Sea Wave Project (JONSWAP). Ergaenzungsheft zur Deutschen Hydrographischen Zeitschrift, Reihe A. 1973.

[16] Zdravković L, Jardine RJ, Taborda DMG, Abadias D, Burd HJ, Byrne BW, et al. Ground characterisation for PISA pile testing and analysis. Géotechnique. 2020;70(11):945-60.

[17] Hardin BO, Black WL. Vibration Modulus of Normally Consolidated Clay. Journal of the Soil Mechanics and Foundations Division. 1968;94(2):353-69.

[18] Byrne BW, McAdam RA, Burd HJ, Beuckelaers WJAP, Gavin KG, Houlsby GT, et al. Monotonic laterally loaded pile testing in a stiff glacial clay till at Cowden. Géotechnique. 2020;70(11):970-85.

[19] Zdravković L, Taborda DMG, Potts DM, Abadias D, Burd HJ, Byrne BW, et al. Finite-element modelling of laterally loaded piles in a stiff glacial clay till at Cowden. Géotechnique. 2020;70(11):999-1013.

[20] Arany L, Bhattacharya S, Macdonald J, Hogan SJ. Design of monopiles for offshore wind turbines in 10 steps. Soil Dynamics and Earthquake Engineering. 2017 jan;92:126-52.

[21] Ryan GV, Adcock TAA, McAdam RA. Influence of soil plasticity models on offshore wind turbine response. Wind Energy. 2024;27(2):131-51.

[22] Miner MA. Cumulative Damage in Fatigue. Journal of Applied Mechanics. 2021 03;12(3):A159-64.

[23] Veritas DN, Lloyd G. Fatigue design of offshore steel structures. DNV GL; 2019. DNV-RP-C203.

[24] Porté-Agel F, Bastankhah M, Shamsoddin S. Wind-Turbine and Wind-Farm Flows: A Review. Boundary-Layer Meteorology. 2020 jan;174(1):1-59.

[25] Feng J, Shen WZ. Modelling Wind for Wind Farm Layout Optimization Using Joint Distribution of Wind Speed and Wind Direction. Energies. 2015;8(4):3075-92.

[26] Patel K, Dunstan TD, Nishino T. Time-Dependent Upper Limits to the Performance of Large Wind Farms Due to Mesoscale Atmospheric Response. Energies. 2021;14(19).

[27] Nishino T, Dunstan TD. Two-scale momentum theory for time-dependent modelling of large wind farms. Journal of Fluid Mechanics. 2020;894.

[28] Legris L, Pahus ML, Nishino T, Perez-Campos E. Prediction and Mitigation of Wind Farm Blockage Losses Considering Mesoscale Atmospheric Response. Energies. 2023;16(1).

[29] Kirby A, Nishino T, Dunstan TD. Two-scale interaction of wake and blockage effects in large wind farms. Journal of Fluid Mechanics. 2022;953:1-28.

[30] Alkhoury P, Soubra AH, Rey V, Aït-Ahmed M. A full three-dimensional model for the estimation of the natural frequencies of an offshore wind turbine in sand. Wind Energy. 2021;24(7):699-719.